Parameter optimization and experiment of the negative pressure precision seed-metering device for wheat

Yubo Feng[1,2], Xiaoshun Zhao[1,2*], Jincai Li[1], Huali Yu[2], Hongpeng Zhao[2], Baozhong Yin[3]

(1. *State Key Laboratory of North China Crop Improvement and Regulation, Hebei Agricultural University, Baoding 071001, Hebei, China*;
2. *College of Mechanical and Electrical Engineering, Hebei Agricultural University, Baoding 071001, Hebei, China*;
3. *College of Plant Protection, Hebei Agricultural University, Baoding 071001, Hebei, China*)

Abstract: In order to ensure the most reasonable distribution of wheat seeds in the field to improve seeding quality and uniformity, a set of negative pressure precision seed-metering device was designed, which shares a hollow shaft. Every seed-metering device can sow two rows of wheat. By the STAR-CCM+, the analysis of nephogram, vectogram and streamline graph showed that more ideal structural parameters of the seed-metering device are 0.5 mm width of the slit sucking seed (WSS), 150-200 mm diameter of the seed-metering disc (DSD), 2.0 mm axial depth of air chamber in the seed-metering disc (ADS), and arc-shaped cross-section shape of the ring groove sucking seed (CSGS). Single-factor test on the JPS-12 test-bed analyzed the influence of the CSGS, WSS, DSD, and ADS on the qualified index (I_q), multiple index (I_{mul}), miss index (I_{miss}) and coefficient of variation of qualified seed spacing (CV). Through the orthogonal on the JPS-12 test-bed, it is found that the influence of vacuum negative pressure and seed-metering device shaft speed is significant on the I_q, I_{miss} and I_{mul}. Based on these, the structural parameters of the seed-metering device were optimized. The DSD is 180 mm, the WSS is 0.7 mm, the ADS is 2.5 mm, and the CSGS is arc-shaped. The optimization seed-metering device was tested on the JPS-12 test-bed. The I_q is 86.66%, the I_{miss} is 5.09%, the I_{mul} is 8.25%, and the CV is 24.50%. These testing results fully coincide with the standard JB/T 10293-2013 Specifications of single seed drill (precision drill). The seed-metering device meets fully the requirements for wheat precision seeding.

Keywords: wheat, seed-metering device, negative pressure, precision, parameter optimization, STAR-CCM+, orthogonal test, variance analysis

DOI: 10.25165/j.ijabe.20241701.8222

Citation: Feng Y B, Zhao X S, Li J C, Yu H L, Zhao H P, Yin B Z. Parameter optimization and experiment of the negative pressure precision seed-metering device for wheat. Int J Agric & Biol Eng, 2024; 17(1): 154–162.

1 Introduction

Wheat precision seeding technology ensures the most reasonable distribution of wheat seeds in the field through precisely controlling seeding quantity and uniformity. It makes each grain of wheat seed get enough nutritional area and space, absorbs the most water and possess effective tillering. It ensures stable and high yield under seed-saving, fertilizer-saving and water-saving conditions, and huge economic benefits and social benefits can be obtained[1,2]. In order to realize wheat precision seeding technology, the precision seed-metering device plays a crucial role. It limits the uniformity of wheat precision seeding, the practicality of the whole machine and the popularization[3,4].

At present, foreign air suction seed-metering device is a common device for precision seeding, which is widely used in the seeder of maize, soybean and other crops[5-9]. It is less used for small grain sowing in lines for wheat. Foreign mature seeder includes Germany Lemken air suction precision seeder, Solitair 9 series seeder, Matt Mark negative pressure grain seeder, et al.[10,11]. But the seeder is huge and expensive, which is not suitable for the domestic market[12-14]. In China, the combined suction hole type seed-metering device had been experimental research[15-18]. Bai et al.[19] designed an air suction pressure precision seed-metering device. Liu et al.[20] studied and manufactured air suction precision seeder, and conducted experiments. A hole-tube air suction wheat seeder was studied[21-24]. However, the seed-metering device structures mentioned above are hole-tube air suction. This form of seed-metering device is prone to blockage, poor seed arrangement uniformity and other defects. Therefore, a pressure precision seed-metering device for wheat with good seed arrangement uniformity, high stability and not prone to blockage is designed. It takes the traditional over a certain width crowded dense wheat strip sowing band into a line sowing band. Because the distribution of wheat seeds in the field is more reasonable, it can absorb fertilizer, water and nutrients to the maximum extent, the utilization rate of fertilizer and water has been improved, effective tiller more, water-saving and fertilizer-saving while ensuring stable wheat production. To further promote the development of wheat precision seeding agronomic technology and provide a reference for the study of wheat precision seeder suitable for Chinese agricultural production.

Received date: 2023-03-06 **Accepted date:** 2024-01-04

Biographies: **Yubo Feng**, MS candidate, research interest: agricultural mechanization engineering, Email: fengyubo169@163.com; **Jincai Li**, PhD, Professor, research interest: crop cultivation, Email: kjzl@hebau.edu.cn; **Huali Yu**, MS, research interest: vehicle engineering, Email: 48796619@qq.com; **Hongpeng Zhao**, MS candidate, research interest: agricultural mechanization engineering, Email: zhp18132725947@163.com; **Baozhong Yin**, PhD, Associate Professor, research interest: physiological ecology of crop stress resistance, Email: yinbaozhong@hebau.edu.cn.

***Corresponding author: Xiaoshun Zhao**, PhD, Associate Professor, research interest: modern agricultural equipment design and control, precision planting technology. College of Mechanical and Electrical Engineering, Hebei Agricultural University, Baoding 071001, Hebei, China. Tel: +86-13630851145, Email: zhao_xsh@126.com.

2 Materials and methods

2.1 Structure and working principle of the seed-metering device

The seed-metering device is mainly composed of shell of the seed-metering device, board to control seed height, block to stop seed, device falling seed and clearing, negative pressure hollow shaft, rotating seed-metering disc I, rotating seed-metering disc II, Immobile seed-metering disc, Fixed sleeve, Joint block to control gap, Joint screw, etc., as shown in Figure 1.

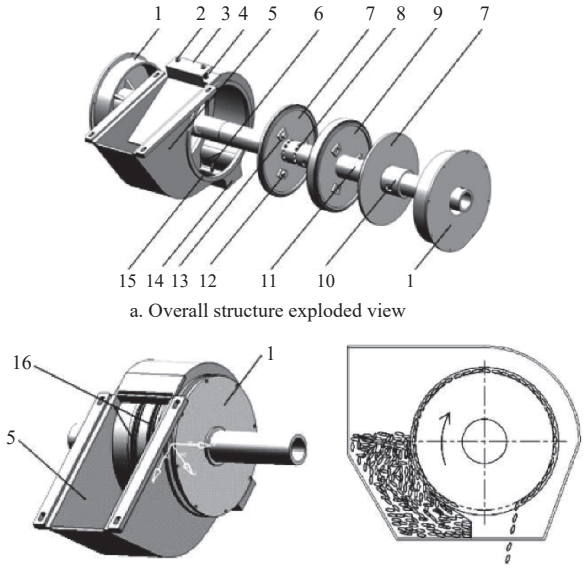

a. Overall structure exploded view

b. Overall structure assembly drawing c. Operating principle diagram

1. Immobile seed-metering disc 2. Nuts 3. Board to control seed height 4. Spring 5. Shell of seed-metering device 6. Device falling seed and clearing jams 7. Rotating seed-metering disc Ⅰ 8. Air hole 9. Rotating seed-metering disc Ⅱ 10. Fixed sleeve 11. Negative pressure hollow shaft 12. Jiont screw 13. Jiont block to control gap 14. Seed-metering opening 15. Block to stop seed 16. Ring groove sucking seed and slit sucking seed

Figure 1 Structure and working principle diagram of the seed-metering device

The two sides of the rotating seed-metering disc II are recessed to form half a negative pressure chamber, and the rotating seed-metering disc I side near the rotating seed-metering disc Ⅱ is concave to form another half negative pressure chamber. Connect the fan connection hose to the negative pressure hollow shaft of the seed-metering device through the rotary joint. The negative pressure hollow shaft processes at the equal spacing through-hole array in the circular direction of the negative pressure chamber formed by the two rotating seed-metering discs. In this way, an airflow path is formed from the atmospheric pressure of the outer edge of the seed-metering disc to the fan. The airflow flows from the outer edge of the seed-metering disc to the inside. During the rotation of the seed-metering disc, the wheat seed is adsorbed along the outer circle direction and forms a circular seed band. In the unstable area, the wheat seed in the seed box is adsorbed in the ring groove sucking seed belt outside the seed-metering disc by negative pressure suction and rotates through the stable area to reach the falling seed area. In the falling seed area, the device falling seed and clearing jams cut off the air suction or reduce the airflow suction in advance, and the wheat seed freely falls into the seed tube under the action of gravity. In addition, the device falling seed and clearing jams is located in the slit sucking seed of the rotating seed-metering disc, so it can remove the sucked wheat impurities in the gap, preventing the slot from becoming blocked after long-term work.

2.2 Finite element analysis steps and boundary conditions setting

SolidWorks was used to establish the 3D model for the seed-metering device, import the seed-metering device model into the finite element analysis software STAR-CCM+, and select the polyhedral grid type. Physical model parameters are set as 3D steady-state computational model, separation solver, and the fluid domain of air with fixed constant density in the standard k-ε turbulence model. The boundary conditions are set to: one standard atmospheric pressure, the value of the pressure outlet is −22 kPa (The JPS-12 seed-metering device tester provides 80% of the maximum negative pressure value, and the value is an integer). Establish the rotation model and parameters (80 r/min speed, the design maximum speed of the seed-metering device), and apply it to the entire fluid domain model to simulate the actual working rotation scene of the seed-metering device.

2.3 JPS-12 seed-metering device test arrangement and method

2.3.1 Test materials, test equipment and evaluation indicators

The wheat grain material used in the test was Shixin 828: the average length is 6.26 mm, the average width is 3.53 mm, the average thickness is 3.12 mm and the 1000 grain mass is 40.90 g. Seed-metering device with different structural parameters processed with nylon rod. The test equipment is the JPS-12 seed-metering device test bench, as shown in Figure 2.

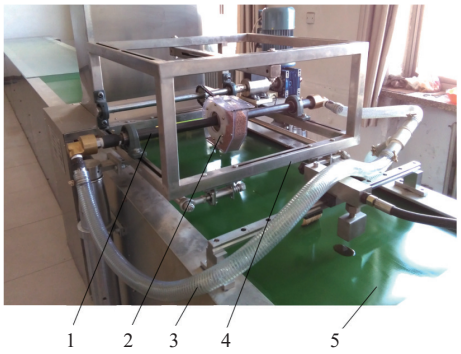

1. Seed-metering device shaft 2. Seed-metering device 3. Air tube 4. Seed-metering device holder 5. Conveyor belt

Figure 2 JPS-12 seed-metering device test bench

Four structural parameters, including WSS, CSGS, DSD and ADS, were taken as test factors to analyze the influence of each parameter on the Seed-metering performance and used to verify the computer fluid simulation analysis results. The uniformity of seed arrangement was used as the evaluation index of seed metering performance of seed-metering device to analyze the uniformity of longitudinal distribution of seeds in rows. The JPS-12 test bench can measure the test data required in GB/T6973-2005 Single Seed (Precision drill) Seeder Test Method (2005). The real-time images of performance collecting video of the seed-metering device for wheat seed on the conveyer belt can be obtained (Figure 3a), and the distribution of wheat seed on the conveyer belt can also be analyzed manually (Figure 3b).

According to the national standard GB/T 6973-2005 Single Seed (Precision drill) Seeder Test Method, the seed-metering performance index is I_q, I_{mul}, and I_{miss}; The seed-metering accuracy index is the CV. The test section was 500 particle lengths. The seed-metering device gear speed was set at 10.0 r/min, the conveyer belt speed is 2.0 km/h, and the test negative pressure is –0.9 kPa. The I_q, I_{mul}, I_{miss}, and CV were measured on the JPS-12 test bench, the

experiment was repeated 3 times in each group, and the results were averaged. The calculation equation is as follows:

$$I_q = \frac{n_1}{N'} \times 100\% \quad (1)$$

$$I_{\text{mul}} = \frac{n_2}{N'} \times 100\% \quad (2)$$

$$I_{\text{miss}} = \frac{n_0}{N'} \times 100\% \quad (3)$$

$$\text{CV} = \sqrt{\frac{\sum n_i X_i^2}{n_2'} - \bar{X}^2} \times 100\% \quad (4)$$

where, N' is the determination interval number; n_0 is the miss number; n_1 is the qualified number; n_2 is the multiple number; n_2' is the qualified intervals number; $\bar{X}$ is the average value of qualified seed spacing.

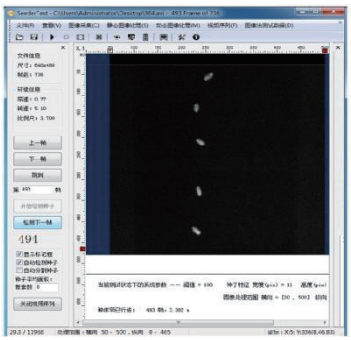

a. Single fps image of performance collecting video of seed-metering device forwheat

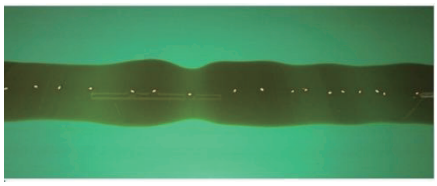

b. Picture of wheat seed distribution on the conveyer belt

Figure 3 Wheat seed distribution and video capturing images

2.3.2 Single-factor test arrangement and method

Single-factor test analyzed the influence of the CSGS, WSS, DSD and ADS on the uniformity of the seed-metering device.

1) Single-factor test of the effect of the CSGS on the uniformity of the seed-metering device. The CSGS determines the permutation posture of the wheat seed being adsorbed on the seed-metering device, and also directly affects the stability of the pressure field and the flow velocity field of the air chamber flow field. The seed-metering device of four structures of straight-groove-shaped, V-shaped, inverted-trapezoid-shaped, and arc-shaped was designed and processed. The seed-metering device is 0.5 mm in WSS, 170.0 mm in DSD, and 2.0 mm in ADS.

2) Single-factor test of the effect of the WSS on the uniformity of the seed-metering device. The CSGS of the seed-metering device is arc-shaped, 170.0 mm DSD, 2.0 mm ADS, and the WSS are 1.0, 2.0, and 3.0 mm, respectively.

3) Single-factor test of the effect of the DSD on the uniformity of the seed-metering device. According to the previous theoretical analysis and computational fluid simulation analysis results, in this experiment, four different DSD of 150 mm, 170 mm, 200 mm, and 250 mm were designed. The seed-metering device is 0.5 mm WSS, and the CSGS is the arc-shaped, 2.0 mm ADS.

4) Single-factor test of the effect of the ADS on the uniformity of the seed-metering device. The results of computational fluid simulation analysis show that the ADS at 2.0 mm is more suitable. Therefore, in this test, three size parameters of the ADS of 1.0, 2.0, 2.0, and 3.0 mm were designed for the comparative test. The CSGS is an arc-shaped, seed-metering device that is 0.5 mm in WSS, and 170.0 mm DSD.

2.3.3 Orthogonal test arrangement and method

The basic structural parameters of the seed-metering device were determined by the above test. However, there are many working parameters affecting the working performance of the seed-metering device. These parameters mainly include row shaft speed, vacuum negative pressure, planting bed belt speed, falling height, etc. According to the test results, the ideal working range of the row shaft speed and the vacuum negative pressure is determined, and the 4 factors 4 levels orthogonal test is designed to determine the optimal combination of test factors when single row seed-metering uniformity is optimal. Orthogonal Table L_{16} (4^5) was selected for the orthogonal test. The orthogonal test factor level schedule is listed in Table 1, and the test protocol is listed in Table 2, and each group of the experiment was repeated 3 times.

Table 1 4 factors and 4 levels of orthogonal schedule

Level	Factor			
	Vacuum negative pressure (U)	Rotation speed of seed metering shaft (V)	Belt speed of seed bed (W)	Height of seed falling (H)
	kPa	r/min	km/h	mm
1	–0.7	8	2	150
2	–0.8	10	4	220
3	–0.9	12	6	300
4	–1.0	14	8	400

Table 2 Orthogonal test scheme

Test number	Level combination	Test condition			
		U/kPa	V/r·min^{-1}	W/km·h^{-1}	H/mm
1	$U_1V_1W_1H_1$	1(–0.7)	1(8)	1(2)	1(150)
2	$U_1V_2W_2H_2$	1(–0.7)	2(10)	2(4)	2(220)
3	$U_1V_3W_3H_3$	1(–0.7)	3(12)	3(6)	3(300)
4	$U_1V_4W_4H_4$	1(–0.7)	4(14)	4(8)	4(400)
5	$U_2V_1W_2H_3$	2(–0.8)	1(8)	2(4)	3(300)
6	$U_2V_2W_1H_4$	2(–0.8)	2(10)	1(2)	4(400)
7	$U_2V_3W_4H_1$	2(–0.8)	3(12)	4(8)	1(150)
8	$U_2V_4W_3H_2$	2(–0.8)	4(14)	3(6)	2(220)
9	$U_3V_1W_3H_4$	3(–0.9)	1(8)	3(6)	4(400)
10	$U_3V_2W_4H_3$	3(–0.9)	2(10)	4(8)	3(300)
11	$U_3V_3W_1H_2$	3(–0.9)	3(12)	1(2)	2(220)
12	$U_3V_4W_2H_1$	3(–0.9)	4(14)	2(4)	1(150)
13	$U_4V_1W_4H_2$	4(–1.0)	1(8)	4(8)	2(220)
14	$U_4V_2W_3H_1$	4(–1.0)	2(10)	3(6)	1(150)
15	$U_4V_3W_2H_4$	4(–1.0)	3(12)	2(4)	4(400)
16	$U_4V_4W_1H_3$	4(–1.0)	4(14)	1(2)	3(300)

3 Results and discussion

3.1 Finite element simulation results and analysis

3.1.1 The effect of the CSGS on air chamber flow field

The cross-section of different shapes greatly affects the flow field stability and the wheat arrangement attitude. The influence of arc-shaped, V-shaped, inverted-trapezoid-shaped, and straight-groove-shaped cross-sections of 4 different suction ring groove sucking seeds (Figure 4a) on the pressure distribution of the airflow field were compared and analyzed. The WSS, DSD, and ADS are

0.5 mm, 170.0 mm, and 2.0 mm respectively. Figure 4b shows a cross-section nephogram under different shape CSGS. As shown in Figure 4b, the CSGS is arc-shaped, V-shaped, inverted-trapezoid-shaped slit sucking seed nephogram is more stable than the straight-groove-shaped, the arc-shaped is similar to the V-shaped, but from the local amplification diagram, the pressure gradient at the entrance of the slit sucking seed of the arc-shaped CSGS is more stable.

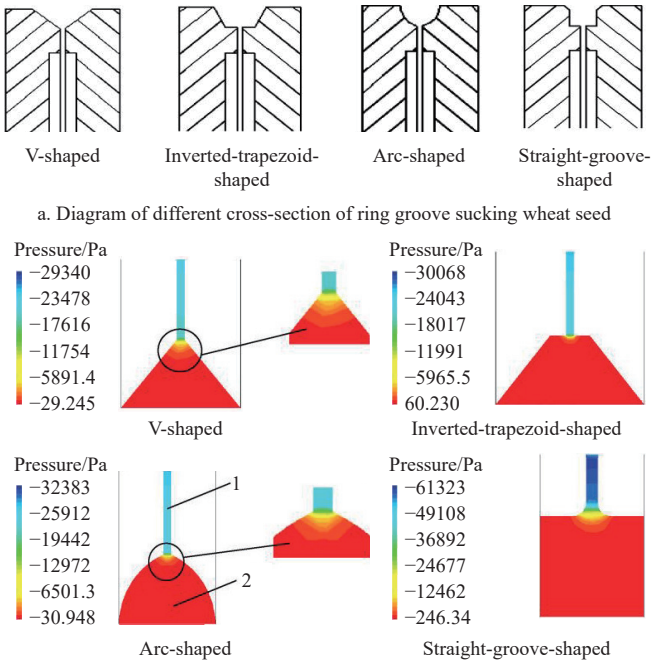

a. Diagram of different cross-section of ring groove sucking wheat seed

b. Cross section pressure nephogram

1. Slit sucking seed 2. Ring groove sucking seed

Figure 4 Cross-section pressure nephogram under different CSGS

3.1.2 Effect of the WSS on air chamber flow field

The size WSS has a great impact on the vacuum degree, the flow velocity stability, and the Power consumption of the fan of the air chamber flow field, Through theoretical calculation and empirical reference, the WSS was preliminarily determined to be 0.45-0.54 mm. Increase the value range appropriately in the computational fluid mechanics simulation analysis. In order to clearly analyze the influence law, four different WSS of 0.3 mm, 0.5 mm, 0.8 mm, and 1.0 mm were set for model analysis. The CSGS is arc-shaped, the DSD is 170.0 mm and the ADS is 2.0 mm. Figure 5a shows the cross-section of nephogram of different widths of the slit sucking seed of seed-metering device models after simulation calculation. As shown in Figure 5a, the pressure at the inlet of the air chamber flow field (Junction between blue area and red area) of the 0.3 mm WSS is very unstable, stress mutations are more obvious. The pressure change in the WSS (blue slender area) is not the change of gradient, the stability is poor. A comparative analysis of Figure 5b shows that as the WSS increases, the unstable pressure area at the WSS entrance increases. When the WSS increases to 1.0 mm, the pressure instability also appears in the suction ring groove sucking seed flow zone area away from the suction slit. From the numerical equivalent column in Figure 5a, The maximum negative pressure values at 1.0, 0.8, 0.5, and 0.3 mm for the gaps are respectively: –34 310 Pa, –42 720 Pa, –63 855 Pa, –58 728 Pa. The suction was maximum in the 0.5 mm WSS. In addition, the pressure field in the 0.5 mm gap changes continuously and smoothly in a gradient, which is more stable than the pressure field in another WSS.

Figure 5b shows the fluid domain flow rate for different WSS, with the maximum flow rate of 310.73 m/s when the WSS is 0.5 mm (numerical equivalent column in Figure 5b), the flow velocity decreases as the WSS increases. Meanwhile, the reflux phenomenon occurs in the fluid domain with the WSS of 0.8 and 1.0 mm (the blue up arrow in Figure 5b), which leads to the fluctuation of the wheat seed and then affects the suction stability. cross-section of nephogram and vectogram: the pressure field of 0.5 mm WSS is uniformly stable, and the vectogram basically lacks the reflux phenomenon, which belongs to the excellent parameter.

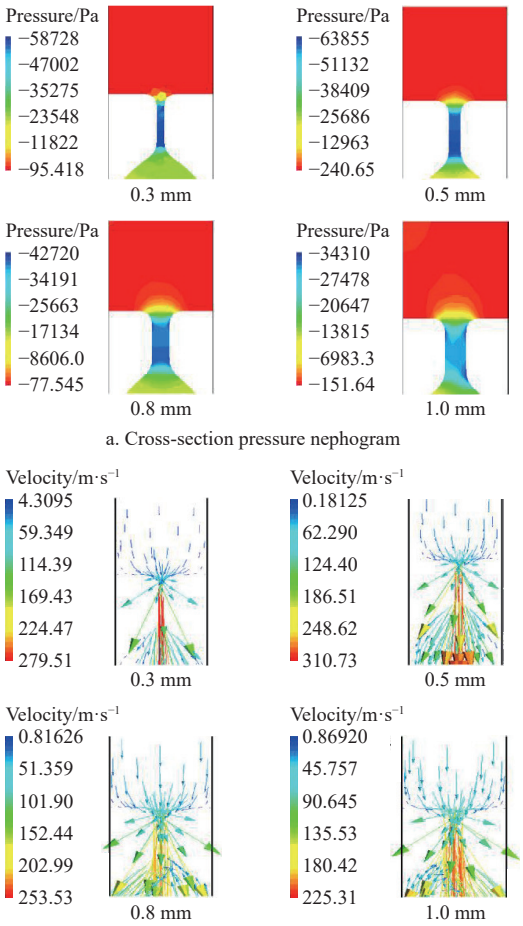

a. Cross-section pressure nephogram

b. Cross-section of velocity vectogram

Figure 5 Cross-section of pressure nephogram and velocity vectogram of air chamber with different WSS

3.1.3 Effect of the DSD on air chamber flow field

The DSD has a relatively large impact on the seed-metering device efficiency and the power consumption of the fan. In the premise of reducing the power consumption of the fan, increase the DSD as far as possible to improve its efficiency of the DSD. The general parameter range of the DSD is between 140-260 mm. In this study, three sizes of DSD models of 150 mm, 200 mm, and 250 mm were selected for fluid simulation calculation to analyze the trend of the influence of the diameter on the vacuum degree of the air chamber flow field. In the seed-metering device, the WSS is 0.5 mm, the CSGS is arc-shaped and the ADS is 2.0 mm. The results are shown in Figure 6. As is seen from Figure 6a, With the increase of the DSD, the absolute value of the maximum negative pressure value at the slit sucking seed (the numerical equivalent column in Figure 6a) shows a decreasing trend; The color of the area near the outlet of the fluid domain (axle hole position) gradually changes from yellow to green, that is, the absolute value of the pressure

difference gradually increases, and the vacuum degree required is increasing, that is, the power consumption of the fan increases under the condition of reaching the same vacuum degree at the slit sucking seed. As is seen from Figure 6b, The larger the DSD, the smaller the absolute value of the pressure difference in the slit sucking seed (the numerical equivalent column in Figure 6b), that is, the lower the vacuum degree; At the same time, pressure fluctuations appeared in the fluid region of the corresponding ring groove sucking seed in the 250 mm DSD (the lower right corner and red inconsistent area in the 250 mm pressure cloud chart in Figure 6b). Considering the work efficiency, power consumption, and specifications of the materials used in processing, the optimal parameter range of the DSD is between 150 and 200 mm.

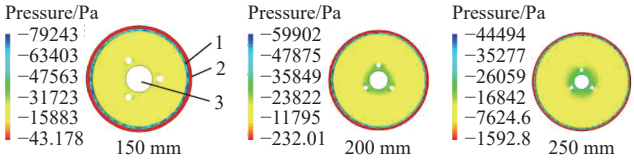

a. Pressure nephogram under different diameter of seed-metering disc

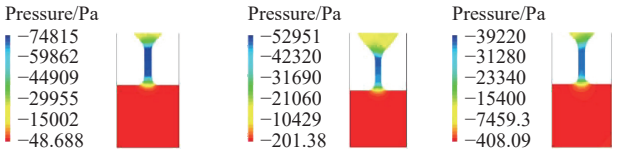

b. Cross section pressure nephogram under different diameter of seed-metering disc

1. Slit sucking seed 2. Ring groove sucking seed 3. Axle hole

Figure 6 Pressure nephogram of air chamber with different DSD

3.1.4 The effect of the ADS on the air chamber flow field

The air chamber in the seed-metering disc is an excessive cavity connecting the gap between the fan and the slit sucking seed. With a certain diameter, the axial depth and shape directly affect the pressure and flow rate of the overall flow field of the seed-metering device. Then, the seed absorption performance of the seed-metering device and the seed arrangement performance are determined. In Figure 7, the ADS model is 1.0, 2.0, and 3.0 mm respectively. In the seed-metering device, the WSS is 0.5 mm, the CSGS is arc-shaped and the DSD is 170 mm. As is seen from Figure 7, The greater the axial depth of the air chamber, the color of the area near the exit of the fluid domain (axial hole position) gradually coincides with the color of the air chamber fluid domain (changing from green to yellow), This indicates that the greater the axial depth of the air chamber, the smaller the absolute value of the pressure difference, That is, the smaller the air resistance. At the same time, the greater the axial depth of the air chamber, the greater the vacuum of the slit sucking seed (Maximum value of the numerical equivalent column in Figure 7c, –88 109 Pa). It can be seen that increasing the ADS is beneficial to reducing air resistance and increasing the gap vacuum degree. However, when the axial depth of the air chamber increase is too large, the WSS varies too much from the CSGS, and the airflow channel changes from narrow to wide, and the reflux phenomenon occurs (Blue reflux arrow in Figure 8), affect the seed suction stability of the seed-metering device. Comprehensive analysis shows that the ADS of 2.0 mm is the better parameter value.

In order to verify the credibility of the fluid simulation model and results, the pressure in the air chamber in the seed-metering dis needs to be monitored. The stability of WSS on air chamber flow field of 0.3, 0.5, 0.8, and 1.0 mm was verified, seed-metering device are 0.5 mm WSS, 170.0 mm DSD, 2.0 mm ADS. Four pressure measuring points are arranged at the interval 90° of the seed disc suction gap, the pressure measuring probe is made of a 1.5 mm diameter needle, and the pressure measuring instrument is the HT-930 from Hongcheng Technology, with an accuracy of ±0.3%. Under the pressure corresponding to the simulated data, three pressure values were measured at each measurement point, and then averaged, and the test results are listed in Table 3.

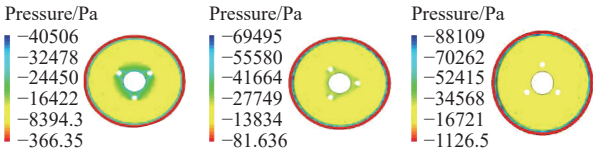

a. 1 mm b. 2 mm c. 3 mm

Figure 7 Pressure nephogram under different ADS

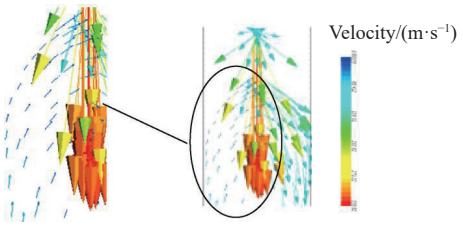

Figure 8 Cross-section velocity vectogram under 3.0 mm ADS

Table 3 Actual testing pressure value in slit sucking seed of seed-metering device

WSS/mm	Testing point 1/kPa	Testing point 2/kPa	Testing point 3/kPa	Testing point 4/kPa
0.3	–48.64	–52.95	–46.36	–50.24
0.5	–59.89	–60.35	–60.60	–59.74
0.8	–39.73	–38.56	–40.99	–41.02
1.0	–32.56	–31.97	–33.53	–30.94

As is seen from Table 3, the pressure value of the 0.5 and 0.8 mm slit is much more stable, and the numerical simulation value and the test value agree well, thus verifying the feasibility of the numerical simulation method.

3.2 JPS-12 seed-metering device test arrangement and method

3.2.1 Single-factor test results and analysis

The uniformity test data of seed-metering device results are listed in Table 4. The seed-metering effect is relatively ideal.

Table 4 Uniformity test data of seed-metering device

Factor	Level	I_q/%	I_{miss}/%	I_{mul}/%	CV/%
CSGS	Arc-shaped	86.43	5.29	8.29	21.47
	V-shaped	76.99	10.06	12.95	25.08
	Inverted-trapezoid-shaped	76.98	5.60	17.41	23.62
	Straight-groove-shaped	69.23	15.52	15.25	29.94
WSS/mm	0.3	69.79	21.88	8.33	24.26
	0.5	82.43	6.69	10.88	23.65
	0.8	83.20	7.38	9.43	25.00
	1.0	52.59	32.60	14.81	26.91
DSD/mm	150	88.88	3.12	8.00	27.96
	170	88.69	5.01	6.31	26.80
	200	84.00	8.43	7.73	21.61
	250	75.31	20.94	3.75	28.43
ADS/mm	1.0	71.43	18.32	10.26	29.25
	2.0	86.11	7.54	6.35	22.76
	3.0	87.34	3.80	8.86	20.16

Single-factor test analyzed the influence of the CSGS, the WSS, the DSD, and the ADS on the uniformity test of the seed-metering device.

1) Single-factor test of the effect of the CSGS on the uniformity of the seed-metering device. The test results are listed in Table 4. By comparative analysis, the arc-shaped I_q has the highest value of 86.43%, the I_{mul}, I_{miss} and CV are low, respectively 5.29%, 8.29% and 21.47%, The I_q of the straight-groove-shaped was the lowest, and the I_{miss} was the highest, with 69.23% and 15.52%, respectively. According to the analysis of test results, the uniformity of the slit sucking seed of the arc-shaped CSGS of the seed-metering device is ideal. The real-time suction effect of the seed-metering device (as shown in Figure 9) qualitatively supports this conclusion.

a. Arc-shaped b. V-shaped c. Inverted-trapezoid-shaped d. Straight-groove-shaped

Figure 9 Sucking seed status picture of seed-metering device with different CSGS

The CSGS on the influence of seed-metering uniformity: arc than V, inverted ladder, straight groove structure I_q is 9.44%, 9.45%, 17.20%, arc groove, and wheat seed shape more fit, smooth and stable airflow, in the row circling through the wheat population, conducive to filling, I_{miss} is low (5.29%), And the wheat seeds along the outer edge of the disk are arranged in the order of the beginning and end of the long diameter line, I_{mul} is low (8.29%).

2) Single-factor test of the effect of the WSS on uniformity of the seed-metering device. The test data are listed in Table 4. It can be seen from the test results that the WSS is in the range of 0.5 to 0.8 mm, and the seed suction effect is relatively ideal. slit sucking seed has a great impact on seed-metering uniformity, under a certain vacuum degree, the reduction of the slit sucking seed (0.3 mm) will make the insufficient adsorption force and affect the absorption effect, resulting in a significant increase in I_{miss} (21.88%), I_q is also very low (69.79%), even wheat seeds cannot be stable adsorption and fall off in the non-stable area.

3) Single-factor test of the effect of the DSD on the uniformity of the seed-metering device. The results are listed in Table 4. The I_q showed a decreasing trend, the I_{miss} increased significantly, the I_{mul} basically showed a decreasing trend, and the CV showed a decreasing trend, but it increased significantly at 250 mm. The change in the DSD has many effects on the seed-metering uniformity. With the increase in the DSD, the pressure difference at the slit sucking seed decreases, and the line speed at the edge increases. As can be seen from the test data, the I_{miss} increases significantly. The results show that with the increase of the DSD, the I_q decreases and the I_{miss} increases significantly. However, in the actual sowing operation, the reduced DSD will reduce the operating efficiency. In the case of the same sowing amount and the same tractor forward speed, the speed of the small DSD will be bound to increase, which will affect the filling performance. Therefore, considering various factors, the DSD is more appropriate to choose at 170-200 mm.

The DSD in the test of less than 200 mm has no impact on the seed-metering uniformity and meets the requirements of precision sowing, However, when increased to 250 mm, the quality of the seed-metering decreased significantly, especially the I_{miss} amount increased significantly (20.94%), The reason is that the DSD increases, the volume of the air chamber increases, the suction at the gap decreases. At the same time, the line speed of the outer edge of the seed-metering disc increases, and the seed filling performance decreased.

4) Single-factor test of the effect of the ADS on the uniformity of the seed-metering device. The results are listed in Table 4. The I_q showed an increasing trend, but did not increase significantly from 2.0 to 3.0 mm, the I_{miss} showed a decreasing trend, and the I_{mul} fell significantly, then slightly higher. In a comprehensive analysis, 2.0-3.0 mm was better than 1.0 mm, and the CV showed a downward trend. From the test results, the ADS in 2.0-3.0 mm was more appropriate.

If the ADS is less than 2.0 mm, the I_q of the seed-metering device will be significantly reduced due to the decrease of vacuum degree, the increase in the I_q was not obvious after exceeding 2.0 mm. However, the axial structure size of the seed-metering device will be limited by the overall structure of the seeder.

3.2.2 Orthogonal test results and analysis

The orthogonal test scheme established for the seed-metering device was done on the JPS-12 test-bed. The three test results of each group were averaged, and the final test results are listed in Table 5. According to the orthogonal test results, the vacuum negative pressure, the rotation speed of the seed metering shaft, the belt speed of the seedbed, and the height of the seed falling are analyzed. According to the national standard GB/T 6973-2005 Single Seed (Precision drill) Seeder Test Method, the seed-metering performance index is the I_q, I_{mul}, I_{miss} and CV.

Table 5 Orthogonal test data

Test No.	U	V	W	H		I_q/%	I_{mul}/%	I_{miss}/%	CV/%
1	1	1	1	1	1	83.83	8.47	7.69	25.82
2	1	2	2	2	2	83.85	7.99	8.16	26.15
3	1	3	3	3	3	82.61	7.81	9.58	27.58
4	1	4	4	4	4	82.57	7.56	9.86	28.78
5	2	1	2	3	4	84.72	9.68	5.61	28.82
6	2	2	1	4	3	83.31	9.48	7.21	28.98
7	2	3	4	1	2	82.48	8.92	8.61	26.89
8	2	4	3	2	1	82.49	8.74	8.77	28.31
9	3	1	3	4	2	83.84	11.03	5.13	29.45
10	3	2	4	3	1	82.49	10.41	7.10	27.41
11	3	3	1	2	4	82.35	9.59	8.05	26.81
12	3	4	2	1	3	82.42	9.02	8.56	25.87
13	4	1	4	2	3	81.93	12.98	5.09	28.45
14	4	2	3	1	4	81.54	12.64	5.82	27.98
15	4	3	2	4	1	81.38	11.19	7.43	28.89
16	4	4	1	3	2	80.51	11.12	8.37	28.69

According to the analysis and comparison of the extreme difference values in Table 6, the I_q of the seed-metering device is affected by various factors: U, V, W and H. Vacuum negative pressure is the first factor affecting the I_q of the seed-metering device, and the influence of the rotation speed of the seed-metering shaft is secondary. The better level combination of the factors in the I_q from the extreme difference perspective is $U_2V_1W_2H_4$. However, the extreme difference analysis cannot distinguish whether the

differences in the corresponding test results between the levels of the factors are caused by the different factor levels or by the trial error, making it impossible to estimate the size of the trial error. Therefore, further analysis of the influence of various factors on the fluctuation and significant status of the I_q is needed. In order to improve the sensitivity of the test, the sum of squares of deviations and degrees of freedom of the obviously insignificant factor H is incorporated into the sum of the error as the sum of squares of deviations and degrees of freedom of the new error. Table 7 lists the results of variance analysis for the I_q. It can be seen in the table that the influence of vacuum negative pressure and rotation speed of the seed metering shaft on the I_q is highly significant, and the optimization level of both types is U_2 and V_1 respectively. The belt speed of the seedbed and the height of the seed falling are not significant. In practice, W_4 should be selected to improve the sowing efficiency, but combined with the analysis results of Tables 6 and 7, I_{mul}, W_2 should be selected. The height of seed falling should H_1 selected according to the controllability principle and the CV in Tables 6 and 8. Therefore, the better level combination of the factors in the I_q is $U_2V_1W_2H_1$.

Table 6 The range analysis table

Terms	I_q/%				I_{mul}/%				I_{miss}/%				CV/%			
	U	V	W	H	U	V	W	H	U	V	W	H	U	V	W	H
K_1	332.86	334.32	330.00	330.27	31.83	42.16	38.66	39.05	35.29	23.52	31.32	30.68	108.33	112.54	110.30	106.56
K_2	333.00	331.19	332.37	330.62	36.82	40.52	37.88	39.30	30.20	28.29	29.76	30.07	113.00	110.52	109.73	109.72
K_3	331.10	328.82	330.48	330.33	40.05	37.51	40.22	39.02	28.84	33.67	29.30	30.66	109.54	110.17	113.32	112.50
K_4	325.36	327.99	329.47	331.10	47.93	36.44	39.87	39.26	26.71	35.56	30.66	29.63	114.01	111.65	111.53	116.10
k_1	83.22	83.58	82.50	82.57	7.96	10.54	9.67	9.76	8.82	5.88	7.83	7.67	27.08	28.14	27.58	26.64
k_2	83.25	82.80	83.09	82.66	9.21	10.13	9.47	9.83	7.55	7.07	7.44	7.52	28.25	27.63	27.43	27.43
k_3	82.78	82.21	82.62	82.58	10.01	9.38	10.06	9.76	7.21	8.42	7.33	7.67	27.39	27.54	28.33	28.13
k_4	81.34	82.00	82.37	82.78	11.98	9.11	9.97	9.82	6.68	8.89	7.67	7.41	28.50	27.91	27.88	29.03
R	1.91	1.58	0.72	0.21	4.02	1.43	0.59	0.07	2.14	3.01	0.50	0.26	1.42	0.60	0.90	2.39
Better combination	$U_2V_1W_2H_4$				$U_1V_4W_2H_1$				$U_4V_1W_3H_4$				$U_1V_3W_2H_1$			
Primary and secondary order	$U>V>W>H$				$U>V>W>H$				$V>U>W>H$				$H>U>W>V$			

Note: K_1, K_2, K_3, and K_4 in the table represent the data of each factor column and the data of the corresponding levels (1,2,3,4); k_1, k_2, k_3, and k_4 represent the comprehensive average of the data at each level; R represents extremely poor.

Table 7 Variance analysis table

Index	Source of variance	Sum of square S	Degrees of freedom	Mean square sum $\bar{S}$	F	F_α	Significance
I_q/%	U	9.643	3	3.214	73.05	F0.05(3,6)=4.76	**
	V	6.041	3	2.014	45.77	F0.01(3,6)=9.78	**
	W	1.196	3	0.399	9.07		
	H^Δ	0.108	3	0.036			
	Error e	0.155	3	0.052			
	e^Δ	0.263	6	0.044			
I_{mul}/%	U	34.227	3	11.409	877.62	F0.05(3,6)=4.76	**
	V	5.243	3	1.748	134.46	F0.01(3,6)=9.78	**
	W	0.879	3	0.293	22.54		**
	H^Δ	0.015	3	0.005			
	Error e	0.061	3	0.020			
	e^Δ	0.076	6	0.013			
I_{miss}/%	U	9.981	3	3.327	36.56	F0.05(3,6)=4.76	**
	V	22.257	3	7.419	81.53	F0.01(3,6)=9.78	**
	W	0.614	3	0.205	2.25		
	H^Δ	0.192	3	0.064			
	Error e	0.353	3	0.118			
	e^Δ	0.545	6	0.091			

Table 8 Variance analysis table of coefficient of variation of qualified seed spacing

Source of variance	Sum of square S	Degrees of freedom	Mean square sum $\bar{S}$	F	F_α	Significance
U	5.532	3	1.844	10.49	F0.05(3,6)=9.23	*
V	0.880	3	0.293	1.67	F0.01(3,3)=29.5	
W	1.893	3	0.631	3.59		
H	12.355	3	4.118	23.42		*
Error e	0.528	3	0.176			

According to the analysis and comparison of extreme difference values in Table 6, the I_{mul} of the seed-metering device is influenced by various factors by vacuum U, V, W and H. Vacuum negative pressure is the first factor affecting the I_{mul} of the seed-metering device, and the influence of rotation speed of seed metering shaft is secondary. The better level combination of the I_{mul} from the extremely poor perspective is $U_1V_4W_2H_1$. The sum of squares of deviations and degrees of freedom of the obviously insignificant factor H is incorporated into the sum of the error as the sum of squares of deviations and degrees of freedom of the new error. Table 7 lists the results of variance analysis for the specifier I_{mul}. It can be seen from the table that the influence of vacuum negative pressure, rotation speed of seed metering shaft and belt speed of seed bed on the I_{mul} is highly significant. The optimization levels of the three are U_1, V_4, and W_2 respectively; while the height of seed falling is not significant. H_1 is selected according to the easy handling principle and the qualified particle distance coefficient of variation in Tables 6 and 8. Therefore, the optimal level combination of the I_{mul} is $U_1V_4W_2H_1$.

According to the analysis and comparison of extreme difference values in Table 6, the order of the seed-metering device I_{miss} that is affected by various factors is V, U, W, and H. The rotation speed of the seed-metering shaft is the first factor affecting the I_{miss} of the seed-metering device, and the influence of vacuum negative pressure is secondary. The better level combination of the factors of the I_{miss} from the extremely poor perspective is $U_4V_1W_3H_4$. Also, the sum of squares of deviations and degrees of freedom of the H are analyzed as the sum of squares of deviations and degrees of freedom of the new error. Table 7 shows the results of variance analysis for the I_{miss} of the seed-metering device. It can be seen from the table that the influence of the rotation speed of the seed metering shaft and the vacuum negative pressure on the I_{miss} is highly significant. The two optimization levels are V_1 and U_4

respectively; while the belt speed of the seedbed and height of seed falling is not significant, so W_2 and H_1 are selected respectively according to the previous analysis conclusions. Therefore, the optimal level combination of the factors in the I_{miss} is $U_4V_1W_2H_1$.

According to the analysis and comparison of extreme difference values in Table 6, the CV of the seed-metering device is affected by various factors: height of seed falling, vacuum negative pressure, belt speed of seedbed, and rotation speed of seed separator. The height of the seed falling is the first factor affecting the qualified particle distance variation coefficient of the seed collector, and the influence of vacuum negative pressure is the second. The better level combination of the coefficient of variation from the perspective is $U_1V_3W_2H_1$. Table 8 lists the results of the variance analysis for the coefficient. It can be seen from the table that the influence of the height of seed falling and vacuum negative pressure on the variation coefficient of qualified particle distance is significant, and the optimization level of both species is H_1 and U_1 respectively; However, the belt speed of seedbed and rotation speed of seed metering shaft was not significant, and W_2 and V_1 were selected respectively according to the previous analysis. Therefore, the optimal level combination of the CV is $U_1V_1W_2H_1$.

Through the orthogonal test of seed-metering device uniformity, it is found that the influence of vacuum negative pressure and seed-metering device shaft speed is significant on the I_q, I_{miss} and I_{mul}, and these two factors should be controlled in the actual operation; The effect of belt speed of seed bed on the I_{mul} is also very significant; the influence of vacuum negative pressure and height of seed falling on the CV is very significant.

3.3 Test performance of optimized seed-metering device

Comprehensive simulation analysis and bench test results can determine the ideal structural parameters of the CSGS is arc-shaped, the WSS of 0.5-0.8 mm, the DSD of 170-200 mm, and the ADS of 2.0-3.0 mm. On this basis, the seed-metering device is tried and produced. The structural parameters are as follows: The seed-metering device is 0.7 mm WSS, 180 mm DSD, 2.5 mm ADS, the CSGS is arc-shaped. The arrangement uniformity test of the optimized shaping seed-metering device is also conducted. The tests were performed in triplicate and averaged, and the final test results are listed in Table 9. The test results meet the index parameters of precision sowing performance requirements in JB/T 10293-2013 Specifications of single seed drill (precision drill) (2001).

Table 9 Test performance indicators of optimized seed-metering device

Test No.	I_q/%	I_{mul}/%	I_{miss}/%	CV/%
1	87.60	7.85	4.55	24.72
2	86.07	8.20	5.74	24.56
3	86.31	8.71	4.98	24.21
Average value	86.66	8.25	5.09	24.50

4 Conclusions

1) The precision seed-metering device for wheat by using the principle of vacuum negative pressure is composed of multiple seed-metering units that share a hollow shaft. It effectively solves the problem of uniformity in the traditional wheat picking method. It disperse the wheat seeds crowded in a linear sowing-belt to a certain width of the sowing-belt, so as to achieve precision sowing of wheat.

2) The simulation analysis of the seed-metering device structural parameters by STAR-CCM+ software shows that the ideal structural parameters include 0.5 mm WSS, 150-200 mm DSD, 2.0 mm ADS and the arc-shaped CSGS.

3) The structure parameters of the seed-metering were optimized on the JPS-12 seed-metering test bench. Through the Single-factor test, the structural parameters range of the seed-metering device is: the arc-shaped CSGS, the WSS of 0.5-0.8 mm, the DSD of 170-200 mm, and the ADS of 2.0-3.0 mm. By orthogonal experiment, the optimal combination of each experimental factor was determined based on the analysis of range and variance of orthogonal test data, when the uniformity of single row seed arrangement, the I_q is $U_2V_1W_2H_1$, the I_{mul} is $U_1V_4W_2H_1$, the I_{miss} is $U_4V_1W_2H_1$, the CV is $U_1V_1W_2H_1$. It is found that the influence of vacuum negative pressure and seed-metering device shaft speed is significant on the I_q, I_{miss} and I_{mul}, and these two factors should be controlled in the actual operation.

4) Comprehensive simulation analysis and bench test results can determine the ideal structural parameters is 0.7 mm WSS, 180 mm DSD, the arc-shaped CSGS , 2.5 mm ADS. The I_q is 86.66%, the I_{miss} is 5.09%, the I_{mul} is 8.25%, and the CV is 24.50%. The performance of the parameter-optimized seed-metering device meet the industry standard JB/T 10293-2013 Specifications of a single seed drill (precision drill) and agronomic requirements for precision sowing of wheat.

Acknowledgements

This work was financially supported by the State Key Laboratory of North China Crop Improvement and Regulation (Grant No. NCCIR2024ZZ-12); The Sci-Tech Program of Hebei (Grant No. 23567601H); The Central Government Guides Local Funds for Scientific and Technological Development (Grant No. 236Z7202G); Hebei Province Agriculture and rural Department scientific and technological achievements promotion project plan (Grant No. Jinongke22016).

[References]

[1] Hu H N, Lu C Y, Wang Q J, Li H W, He J, Xu D J, et al. Influences of wide-narrow seeding on soil properties and winter wheat yields under conservation tillage in North China Plain. Int J Agric & Biol Eng, 2018; 11(4): 74–80.

[2] Li Y M, Chandio F A, Ma Z, Lakhiar I A, Sahito A R, Ahmad F, et al. Mechanical strength of wheat grain varieties influenced by moisture content and loading rate. Int J Agric & Biol Eng, 2018; 11(4): 52–57.

[3] Liao Q X, Yang B, Li X, Liao Y T, Zhang N. Simulation and experiment of inside-filling air-blow precision metering device for rapeseed. Transactions of the CSAM, 2012; 43: 51–54.

[4] Yang S D, Zhang D X, Diao P S, Guo Z D, Song W L, Zhang X D. Design and experiment of side positive pressure seed metering device. Transactions of the CSAE, 2015; 31(1): 8–13.

[5] Liao Q X, Zhang P L, Liao Y T, Yu J J, Cao X Y. Numerical simulation on seeding performance of centrifugal rape-seed metering device based on EDEM. Transactions of the CSAM, 2014; 45(2): 109–114.

[6] Wang Y C, Sun H, Li B Q, Han X, Chen H T. Design and experiment of centralized belt type soybean seed-metering device. Transactions of the CSAM, 2019; 50(7): 74–83. (in Chinese)

[7] Li J H, Lai Q H, Zhang H, Zhang Z G, Zhao J W, Wang T T. Suction force on high-sphericity seeds in an air-suction seed-metering device. Biosystems Engineering, 2021; 211: 125–140.

[8] Zhao X S, Yu F C, Zhao D W, Yu H L. Study on the performance test of pneumatic corn precision seed-metering device. Journal of Hebei Agricultural University, 2020; 43(5): 103–107.

[9] Hu H J, Zhou Z L, Wu W C, Yang W H, Li T, Chang C, et al. Distribution characteristics and parameter optimisation of an air-assisted centralised seed-metering device for rapeseed using a CFD-DEM coupled simulation. Biosystems Engineering, 2021; 208: 246–259.

[10] Arzu Y, Adnan D. Measurement of seed spacing uniformity performance

of a precision metering unit as function of the number of holes on vacuum plate. Measurement, 2014; 56(8): 128–135.

[11] Sapkota T B, Majumdar K, Jat M L, Kumar A, Bishnoi D K, McDonald A J, et al. Precision nutrient management in conservation agriculture based wheat production of Northwest India: Profitability, nutrient use efficiency and environmental footprint. Field Crops Research, 2014; 155(14): 233–244.

[12] Lei X L, Hu H J, Wu W V, Liu H N, Liu L Y, Yang W H, et al. Seed motion characteristics and seeding performance of a centralised seed metering system for rapeseed investigated by DEM simulation and bench testing. Biosystems Engineering, 2021; 203: 22–33.

[13] Li M, Ding Y C, Liao Q X, Wang X L. Design of loss sowing detection system for rapeseed pneumatic precision metering device. Journal of Shenyang Agricultural University, 2020; 51(2): 185–191.

[14] Zhao Z, Li Y M, Chen J, Zhou H. Dynamic analysis of seeds pick-up process for vacuum-cylinder seeder. Transactions of the CSAE, 2011; 27(7): 112–116.

[15] Ding L, Yang L, Zhang D X, Cui T, Gao X J. Design and experiment of seed plate of corn air suction seed metering device based on DEM-CFD. Transactions of the CSAM, 2019; 50(5): 50–60. doi:10.6041/j.issn.1000-1298. 2019.05.006 (in Chinese)

[16] Liu K, Yi S J. Design and experiment of seeding performance monitoring system for suction corn planter. Int J Agric & Biol Eng, 2019; 12(4): 97–103.

[17] Wang L, Liao Y T, Wang X Y, Xiao W L, Wang B S, Liao Q X. Design and test on distributor device of air-assisted centralized metering device for rapeseed and wheat. Transactions of the CSAM, 2021; 52(4): 43–53.

[18] Gao X J, Cui T, Zhou Z Y, Yu Y B, Xu Y, Zhang D X, et al. DEM study of particle motion in novel high-speed seed metering device. Advanced Powder Technology, 2021; 32(5): 1438–1449.

[19] Bai W J, Li Y, Yu H L, Zhao D W, Li X L, Zhao X S. Design and simulation optimization of positive and negative pressure seed-metering device. Journal of Hebei Agricultural University, 2022; 45(4): 115–122.

[20] Liu S, Lai Q H, Dong J Y, Cao X L. Simulation and experiment of air-blowing precision seed-metering device for Panax notoginseng. Journal of South China Agricultural University, 2019; 40(3): 125–132.

[21] Ma L, Zhang J G. The design of the hole-tube air suction wheat seeder. Journal of Agricultural Mechanization Research, 2010; 32(6): 97–100.

[22] Ibrahim E J, Liao Q X, Lei W, Liao Y T, Lu Y. Design and experiment of multi-row pneumatic precision metering device for rapeseed. Int J Agric & Biol Eng, 2018; 11(5): 116–123.

[23] Zhao X S, Zhang J G, Ma L. Experimentation research of performance of circular tube slit pneumatic precise wheat seed-metering device. Journal of Agricultural University of Hebei, 2013; 36(1): 105–108.

[24] Lai Q H, Sun K, Yu Q X, Qin W. Design and experiment of a six-row air-blowing centralized precision seed-metering device for Panax notoginseng. Int J Agric & Biol Eng, 2020; 13(2): 111–122.